JOC Article

Chemistry of 4-Alkylaryloxenium Ion "Precursors": Sound and Fury Signifying Something?

Michael Novak,*,† Aaron M. Brinster,† Jill N. Dickhoff,† Jeremy M. Erb,† Matthew P. Jones,† Samuel H. Leopold,† Andrew T. Vollman,† Yue-Ting Wang,† and Stephen A. Glover§

Department of Chemistry and Biochemistry, Miami University, Oxford, Ohio 45056, and School of Biological, Biomedical, and Molecular Sciences, Division of Chemistry, University of New England, Armidale, 2351, New South Wales, Australia

novakm@muohio.edu

Received August 23, 2007

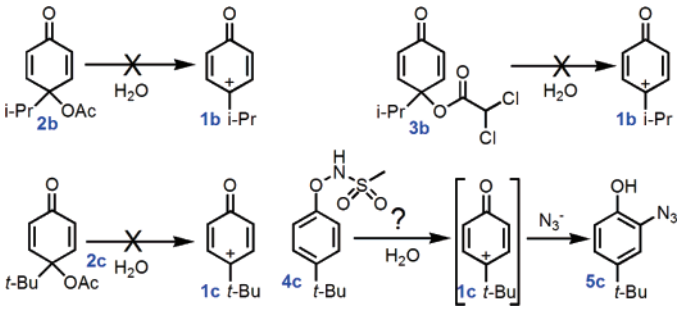

Quinol esters **2b**, **2c,** and **3b** and sulfonamide **4c** were investigated as possible precursors to 4-alkylaryloxenium ions, reactive intermediates that have not been previously detected. These compounds exhibit a variety of interesting reactions, but with one possible exception, they do not generate oxenium ions. The 4-isopropyl ester **2b** predominantly undergoes ordinary acid- and base-catalyzed ester hydrolysis. The 4-*tert*-butyl ester **2c** decomposes under both acidic and neutral conditions to generate *tert*-butanol and 1-acetyl-1,4-hydroquinone, **8**, apparently by an S_N1 mechanism. This is also a minor decomposition pathway for **2b**, but the mechanism in that case is not likely to be S_N1. Decomposition of **2c** in the presence of N_3^- leads to formation of the explosive 2,3,5,6-tetraazido-1,4-benzoquinone, **14**, produced by N_3^--induced hydrolysis of **8**, followed by a series of oxidations and nucleophilic additions by N_3^-. No products suggestive of N_3^--trapping of an oxenium ion were detected. The 4-isopropyl dichloroacetic acid ester **3b** reacts with N_3^- to generate the two adducts 2-azido-4-isopropylphenol, **5b**, and 3-azido-4-isopropylphenol, **11b**. Although **5b** is the expected product of N_3^- trapping of the oxenium ion, kinetic analysis shows that it is produced by a kinetically bimolecular reaction of N_3^- with **3b**. No oxenium ion is involved. The sulfonamide **4c** predominantly undergoes a rearrangement reaction under acidic and neutral conditions, but a minor component of the reaction yields 4-*tert*-butylcresol, **17**, and 2-azido-4-*tert*-butylphenol, **5c**, in the presence of N_3^-. These products may indicate that **4c** generates the oxenium ion **1c**, but they are generated in very low yields (ca. 10%) so it is not possible to definitively conclude that **1c** has been produced. If **1c** has been generated, the N_3^--trapping data indicate that it is a very short-lived and reactive species in H_2O. Comparisons with similarly reactive nitrenium ions indicate that the lifetime of **1c** is ca. 20−200 ps if it is generated, so it must react by a preassociation process. Density functional theory calculations at the B3LYP/6-31G*//HF/6-31G* level coupled with kinetic correlations also indicate that the aqueous solution lifetimes of **1a**−**c** are in the picosecond range.

Introduction

Aryloxenium ions, **1**, have often been invoked to explain a variety of products of the synthetically useful electrochemical and chemical oxidations of phenols[1−5] and the generation of commercially useful polymers such as poly(2,6-dimethyl-1,4-phenylene oxide).[6,7] Until recently these species have received little mechanistic attention. Some examples of stable, highly delocalized **1**, such as **1e** and **1f**, have been observed or

† Miami University.
§ University of New England.

10.1021/jo701853e CCC: $37.00
Published on Web 11/21/2007

isolated,[4,8] but these stable species provide little insight into the reactions of transient members of this class of ions. Previous mechanistic studies of transient ions were not consistent with each other.[9−13] There are discrepancies in the literature concerning the regiochemistry of reaction of purported examples of **1** generated from different sources and the possible involvement of triplet ions.[2,9,11,13]

Recently we have investigated the possibility of generation of **1** in aqueous solution from precursors such as **2**, **3**, and **4** (Scheme 1).[14−16] We have found that oxenium ions with electron-donating 4-aryl substituents such as **1d** can be generated readily from these precursors and their reactions with H_2O and nonsolvent nucleophiles such as N_3^- and Br^- can be characterized. The 4-aryl-substituted ions behave as singlets and have aqueous solution lifetimes that are somewhat shorter than their nitrenium ion analogues.[14−16] Attempts to generate the 4-methyl-substituted ion **1a** from **2a** and **3a** were unsuccessful.[14,15] Although an oxenium-like N_3^--adduct, **5a**, was isolated from the reaction of **3a** with N_3^-, kinetic analysis showed that this product is derived directly from **3a** without the involvement of a transient ion.[15] Calculations and kinetic extrapolations suggest that the 4-alkyl-substituted ions may have aqueous solution lifetimes in the picosecond range, which would make them impossible to detect by nucleophilic trapping experiments and would make alternative bimolecular mechanisms for formation of oxenium-like products competitive.[15,17]

Since many of the examples of possible aryloxenium ion reactions in the literature involve alkyl-substituted ions, we were intrigued by our inability to detect **1a**. As a result we have expanded our study to include the potential precursors **2b**, **2c**, **3b**, **3c**, and **4c**. We reasoned that the steric bulk of the isopropyl or *tert*-butyl groups in **2b**, **2c**, **3b**, and **3c** might enhance the rate of ionization to form **1b** or **1c** if these are accessible species. The precursor **4c** was chosen because of our success with **4d** and related sulfonamides. The compound **3c** was not isolated, but all of the other compounds were synthesized and purified, and their aqueous solution chemistry was examined. Although we discovered a range of interesting reactivities, only one of these compounds, **4c**, exhibits reactions that may be attributable to a transient oxenium ion.

SCHEME 1. Possible Routes to 4-Alkylaryloxenium Ions

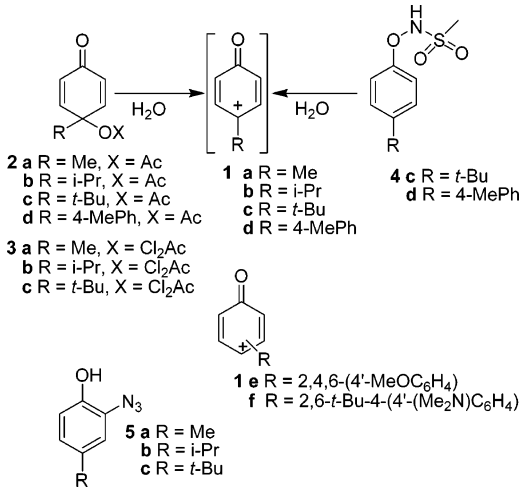

Results and Discussion

All compounds were synthesized by procedures that we have used previously to make **2a**, **3a**, or **4d**.[14−16] All of the target compounds except **3c** were isolated and purified by conventional methods, although **2c** was quite sensitive to acid impurities. Attempts to make **3c** by oxidation of 4-*tert*-butylphenol with phenyliodonium diacetate in dichloroacetic acid led to an intractable tar that did not appear to contain the desired product. The phenol had been consumed, so the oxidation did occur. The synthesis of **3b** was also accompanied by a significant amount of tarry byproduct, but in that case a sufficient amount of the desired product was present so that it could be isolated and purified. Details of synthesis and compound characterization can be found in the Supporting Information.

The reactions of all compounds were followed in 5 vol % CH_3CN-H_2O at $\mu = 0.5$ ($NaClO_4$) in $HClO_4$ solutions (pH < 3.0), or in $HCO_2H/NaHCO_2$, AcOH/AcONa, NaH_2PO_4/Na_2HPO_4, or $TrisH^+$/Tris buffers at 30 °C (**2c**, **3b**), 50 °C (**4c**), or 80 °C (**2b**). Reaction kinetics were monitored as a function of pH because compounds such as **2d** and **4d** typically generate oxenium ions while undergoing pH-independent hydrolysis and, less commonly, acid-catalyzed hydrolysis.[14−16] Pseudo-first-order rate constants for the decomposition of all compounds could be obtained by UV spectroscopic methods or by HPLC. Some compounds, notably **2b** and **4c** (at pH > 8) exhibited distinctly non-first-order UV behavior. This was shown by HPLC to be due to decomposition of initially formed reaction products. In these cases HPLC was used as the primary tool for kinetic analysis. Rate constants smaller than ca. 5×10^{-6} s^{-1} were obtained by initial rates methods.[14] Details of kinetic

(1) (a) Swenton, J. S.; Carpenter, K.; Chen, Y.; Kerns, M. L.; Morrow, G. W. *J. Org. Chem.* **1993**, *58*, 3308−3316. (b) Swenton, J. S.; Callinan, A.; Chen, Y.; Rohde, J. L.; Kerns, M. L.; Morrow, G. L. *J. Org. Chem.* **1996**, *61*, 1267−1274.
(2) Rieker, A.; Beisswenger, R.; Regier, K. *Tetrahedron* **1991**, *47*, 645−654.
(3) Pelter, A.; Ward, R. S. *Tetrahedron* **2001**, *57*, 273−282.
(4) (a) Rieker, A.; Speiser, B.; Straub, H. *DECHEMA Monogr.* **1992**, *125*, 777−782. (b) Dimroth, K.; Umbach, W.; Thomas, H. *Chem. Ber.* **1967**, *100*, 132−141.
(5) Rodrigues, J. A. R.; Abramovitch, R. A.; de Sousa, J. D. F.; Leiva, G. C. *J. Org. Chem.* **2004**, *69*, 2920−2928.
(6) (a) Baesjou, P. J.; Driessen, W. L.; Challa, G.; Reedjik, J. *J. Am. Chem. Soc.* **1997**, *119*, 12590−12594. (b) Driessen, W. L.; Baesjou, P. J.; Bol, J. E.; Kooijman, H.; Spek, A. L.; Reedjik, J. *Inorg. Chim. Acta* **2001**, *324*, 16−20.
(7) Kobayashi, S.; Higashimura, H. *Prog. Polym. Sci.* **2003**, *28*, 1015−1048.
(8) (a) Williams, L. L.; Webster, R. D. *J. Am. Chem. Soc.* **2004**, *126*, 12441−12450. (b) Lee, S. B.; Lin, C. Y.; Gill, P. M.; Webster, R. D. *J. Org. Chem.* **2005**, *70*, 10466−10473.
(9) (a) Abramovitch, R. A.; Inbasekaran, M.; Kato, S. *J. Am. Chem. Soc.* **1973**, *95*, 5428−5430. (b) Abramovitch, R. A.; Alvernhe, G.; Inbasekaran, M. N. *Tetrahedron Lett.* **1977**, 1113−1116. (c) Abramovitch, R. A.; Inbasekaran, M. N. *J. Chem. Soc., Chem. Commun.* **1978**, 149−150. (d) Abramovitch, R. A.; Alvernhe, G.; Bartnik, R.; Dassanayake, N. L.; Inbasekaran, M. N.; Kato, S. *J. Am. Chem. Soc.* **1981**, *103*, 4558−4565.
(10) Li, Y.; Abramovitch, R. A.; Houk, K. N. *J. Org. Chem.* **1989**, *54*, 2911−2914.
(11) (a) Endo, Y.; Shudo, K.; Okamoto, T. *J. Am. Chem. Soc.* **1977**, *99*, 7721−7723. (b) Shudo, K.; Orihara, Y.; Ohta, T.; Okamoto, T. *J. Am. Chem. Soc.* **1981**, *103*, 943−944. (c) Endo, Y.; Shudo, K.; Okamoto, T. *J. Am. Chem. Soc.* **1982**, *104*, 6393−6397.
(12) Uto, K.; Miyazawa, E.; Ito, K.; Sakamoto, T.; Kikugawa, Y. *Heterocycles* **1998**, *48*, 2593−2600.
(13) Hegarty, A. F.; Keogh, J. P. *J. Chem. Soc., Perkin Trans. 2* **2001**, 758−762.
(14) Novak, M.; Glover, S. A. *J. Am. Chem. Soc.* **2004**, *126*, 7748−7749.
(15) Novak, M.; Glover, S. A. *J. Am. Chem. Soc.* **2005**, *127*, 8090−8097.
(16) Novak, M.; Poturalski, M. J.; Johnson, W. L.; Jones, M. P.; Wang, Y.; Glover, S. A. *J. Org. Chem.* **2006**, *71*, 3778−3785.
(17) Glover, S. A.; Novak, M. *Can. J. Chem.* **2005**, *83*, 1372−1381.

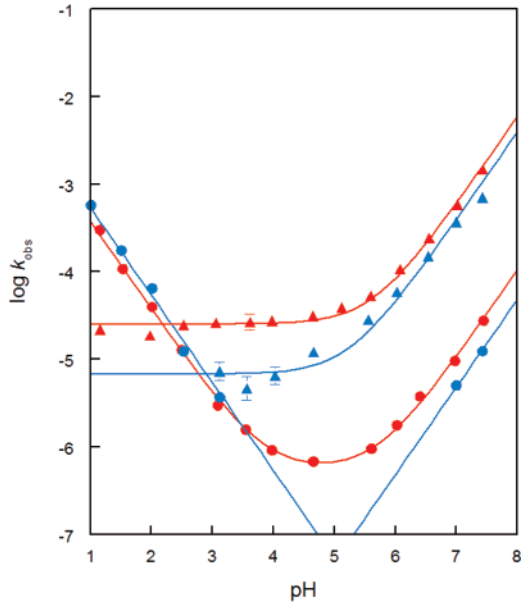

FIGURE 1. Log k_{obs} vs pH for **2a** (red circles), **2b** (blue circles), **3a** (red triangles), and **3b** (blue triangles). Data for **2a** and **3a** were obtained at 80 °C; data for **2b** and **3b** were obtained at 30 °C. Data were fit as described in the text.

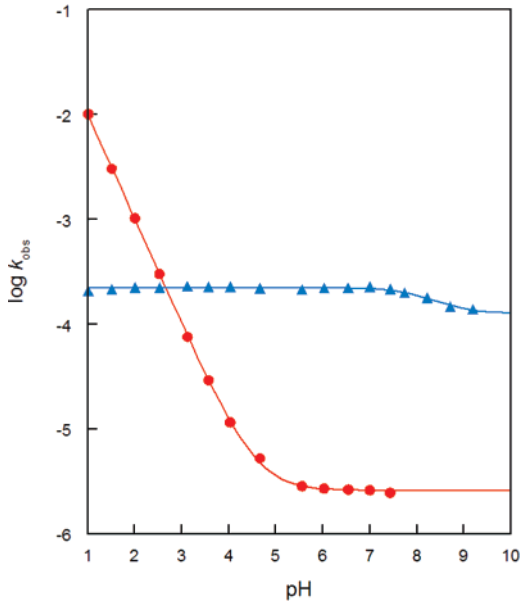

FIGURE 2. Log k_{obs} vs pH for **2c** (red circles) and **4c** (blue triangles). Data for **2c** were obtained at 30 °C; data for **4c** were obtained at 50 °C. Data were fit as described in the text.

methodology can be found in the Experimental Section. In all cases pseudo-first-order rate constants, k_{obs}, could be obtained for the decomposition of each compound under all conditions studied. All individual rate constants are reported in the Supporting Information (Tables S1−S4). The pH dependence of k_{obs} for all compounds is shown in Figures 1 and 2. Previously reported data for **2a** and **3a** are included for comparison purposes.[14,15] The kinetics results, product analyses, and trapping data for each compound are discussed separately below. The kinetic parameters derived for each compound from the fit of log k_{obs} to pH are gathered in Table 1 and discussed below. Previously reported parameters for **2a** and **3a** are included in Table 1 for comparison purposes.[15] All compounds except **2b** do have a significant pH-independent hydrolysis rate constant, k_o, while **2b** and **2c** exhibit acid-catalyzed decomposition.

TABLE 1. Derived Rate Parameters for 2a−c, 3a, 3b, and 4c[a]

compd	temp (°C)	10^3k_H (M^{-1} s^{-1})	10^7k_o (s^{-1})	k_{OH} (M^{-1} s^{-1})	pK_a	10^7k_- (s^{-1})
2a[b]	80	3.8 ± 0.2	5.4 ± 0.5	104 ± 6		
2b	80	5.4 ± 0.4		48 ± 6		
2c	30	100 ± 2	25.8 ± 0.5			
3a[b]	30		266 ± 8	5790 ± 260		
3b	30		68 ± 11	3920 ± 570		
4c	50		2210 ± 20		8.3 ± 0.1	1250 ± 60

[a] All kinetic parameters are defined in the text. [b] Data for **2a** and **3a** come from ref 15.

Kinetically, the isopropyl esters **2b** and **3b** behave similarly to their methyl analogues **2a** and **3a**. The rate data for **2b** and **3b** were fit by nonlinear least-squares methods to eqs 1 and 2, respectively:

$$\text{For 2b: } k_{obs} = k_H[H^+] + k_{OH}[OH^-] \quad (1)$$

$$\text{For 3b: } k_{obs} = k_o + k_{OH}[OH^-] \quad (2)$$

These are the same rate equations, with one additional term, that were used to fit k_{obs} for **2a** and **3a**.[15] The additional parameter for **2a** was a pH-independent rate term (k_o) in eq 1.[15] Since the kinetics for **2b** were not followed in the intermediate pH region where that term would be important, it is not possible to determine whether a pH-independent decomposition also occurs for **2b**. It is clear that there is no significant acceleration of decomposition of **2b** or **3b** compared to **2a** or **3a**. Decomposition of **2a** and **3a** in aqueous solution led to only the corresponding quinol **6a** that subsequently underwent a dienone−phenol rearrangement into **7a** under strongly acidic conditions (Scheme 2).[15] ^{18}O-Labeling experiments showed that **6a** was formed by cleavage of the acyl C−O bond in both **2a** and **3a**, so that both compounds decomposed by ordinary ester hydrolysis mechanisms without the intermediacy of **1a**.[15]

Similarly, **3b** decomposed into **6b** at both pH 4.5 and 7.4 at 30 °C. No other products were detected by HPLC. These pH conditions were chosen because k_o dominates at pH 4.5 and k_{OH} dominates at pH 7.4. At pH 7.4 and 80 °C **2b** also decomposes into **6b**, but at the higher temperature **6b** apparently undergoes a base-catalyzed dienone−phenol rearrangement. The decomposition product of **6b** was not isolated. At pH 1.0 and 80 °C, **2b** predominantly yields **6b** that undergoes decomposition into the same final product, apparently **7b**, observed at pH 7.4. Under these conditions an additional decomposition product of **2b** is detected. Figure 3 shows that **8** is generated at early reaction times as **2b** decomposes. HPLC shows that **8** subsequently decomposes into hydroquinone, **9**, and under the reaction conditions **9** is oxidized to benzoquinone, **10**. This pathway accounts for (32 ± 6)% of the decomposition of **2b** at pH 1.0. Although **8** was not isolated, it was identified by HPLC comparison with an authentic sample of **8**. Authentic **8** also decomposed into **9**, with subsequent oxidation to **10** at pH 1.0 at the same rate as **8** detected in the reaction mixture of **2b**.

Since the isopropyl esters **2b** and **3b** yield reaction products similar to **2a** and **3a**, and with similar rate constants, it appears that these compounds also do not generate an oxenium ion. Confirmation of this conclusion was provided by the results of N_3^- trapping experiments with **3b** at pH 4.5 (Scheme 3). Figure

SCHEME 2. Reaction Products from 2a, 2b, 3a, and 3b

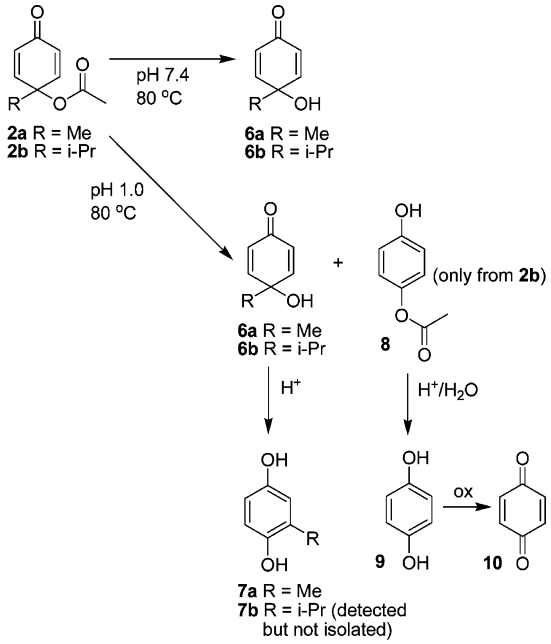

SCHEME 3. Products of the Reactions of 3a and 3b with N_3^-

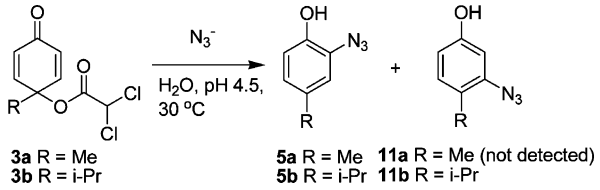

4 shows that decomposition of **3b** in the presence of N_3^- is accompanied by a modest rate acceleration. The observed k_{az}'/k_o is 3.8 ± 0.1 M^{-1}. At 0.25 M N_3^- the N_3^- dependent term, $k_{az}'[N_3^-]$, accounts for (49 ± 2)% of the overall rate of decomposition of **3b**. Under these conditions two isomeric azide products, **5b** and **11b**, are detected by HPLC as shown in Figure 5. The two isomers were distinguished by ^1H and ^{13}C NMR chemical shifts and 2D NMR correlations. NOESY correlations between the aromatic H-3 and H-5 and CH of the isopropyl group in **5b** were particularly helpful. Complete ^1H and ^{13}C NMR assignments for both isomers are provided in the Supporting Information. NMR assignments for **5b** were consistent with analogous assignments previously reported for **5a**.[15] The only other product of decomposition of **3b** is **6b**. All three of these compounds are formed at the same rate at which **3b** decomposes. The combined yield of **5b** and **11b** is (51 ± 3)%, in excellent agreement with the kinetics result. At 0.125 M N_3^- the yield of the azide products predicted by the kinetics data is (32 ± 2)%. The observed combined yield of **5b** and **11b** at 0.125 M N_3^- is (32 ± 3)%. The **5b**/**11b** ratio also remains constant at both concentrations at (1.8 ± 0.1)/1. It appears that both azide products are produced by direct reaction of N_3^- with **3b**. There is no evidence for the involvement of **1b**. This result is similar to that found earlier for **5a** generated from **3a** except

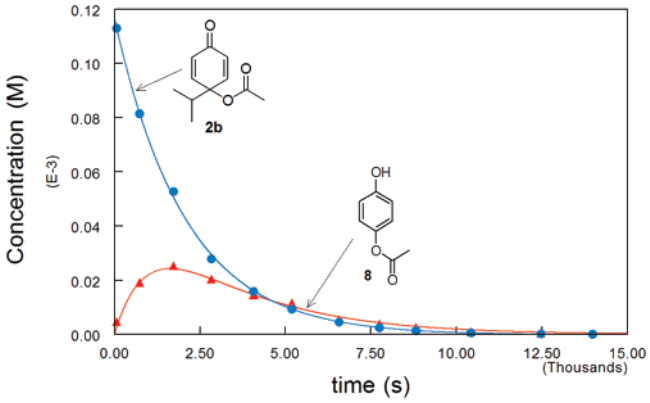

FIGURE 3. Formation and decay of **8** during decomposition of **2b** at pH 1.0 and 80 °C. Concentration vs time data were fit to the first-order rate equation for **2b** and the consecutive first-order rate equation for **8**: k_{obs} = (4.8 ± 0.1) × 10^{-4} s^{-1} for **2b**; k_1 = (3.8 ± 0.6) × 10^{-4} s^{-1} and k_2 = (9.3 ± 1.7) × 10^{-4} s^{-1} for **8**.

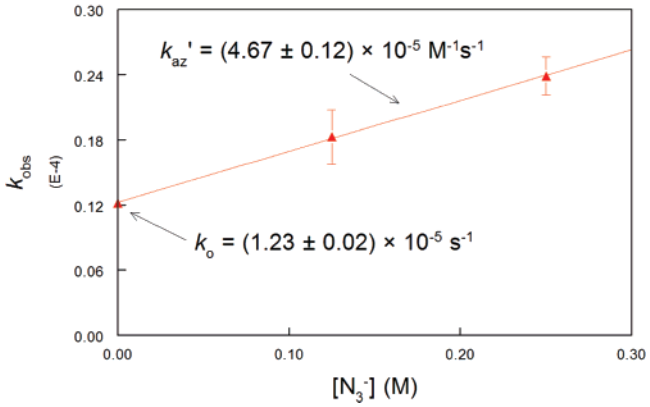

FIGURE 4. Plot of k_{obs} vs $[N_3^-]$ for the decomposition of **3b** in 1/1 N_3^-/HN_3 buffers at pH 4.5 and 30 °C. Rate constants were determined from HPLC data.

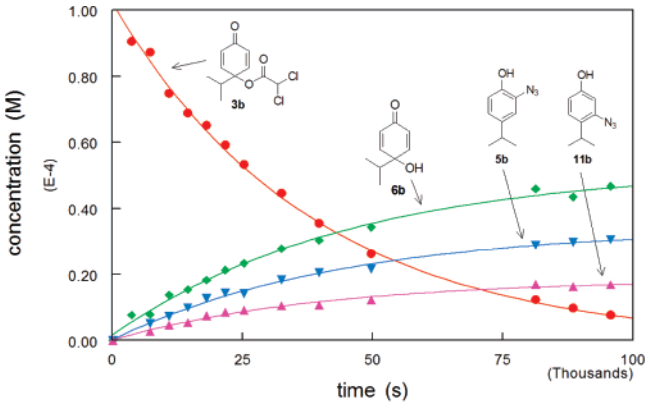

FIGURE 5. Formation of **5b**, **6b**, and **11b** from **3b** in 0.25 M N_3^- at pH 4.5 and 30 °C monitored by HPLC. Data were fit to the first-order rate equation for all compounds.

that in that case the only product observed was **5a**, and N_3^- trapping was more efficient with k_{az}'/k_o = 69 ± 6 M^{-1}.[15] Both **3a** and **3b** mimic aryloxenium ion precursors without actual generation of an oxenum ion.

The product **11b** appears to be formed by a conjugate addition at C-3 to the dienone component of **3b**. An analogous product was not observed during N_3^- trapping of **3a**.[15] The low

SCHEME 4. Products of the Decomposition of 2c

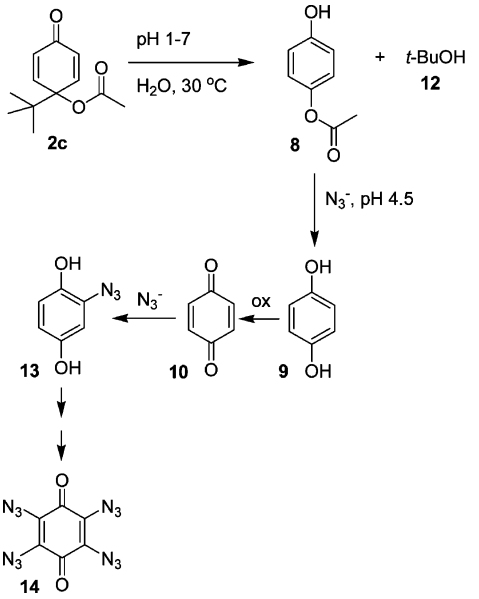

selectivity for reaction with N_3^- exhibited by **3b** may account for this difference. If both compounds have similar reactivity for conjugate addition at C-3, the 18-fold greater reactivity of **3a** would be due to its greater tendency to react at C-2. Then the **5a**/**11a** ratio for **3a** would be ca. 30/1. This would make detection of **11a** unlikely. It is not clear why **3b** is less reactive to N_3^- than **3a**.

Although **2b** decomposes at rates that are very similar to **2a**, the decomposition of **2c** under acidic conditions is significantly accelerated (Figure 2). At pH 1.0 and 30 °C, **2c** decomposes 26-fold more rapidly than **2a** does at the same pH at 80 °C. Rate data for **2c** were fit to eq 3.

$$\text{For } \mathbf{2c}\text{: } k_{obs} = k_H[H^+] + k_o \quad (3)$$

The uncatalyzed decomposition is also accelerated. The rate constant for uncatalyzed decomposition of **2c** at 30 °C (k_o) is 4.8-fold larger than k_o observed for **2a** at 80 °C. The only reaction product detected by HPLC in >95% yield from the decomposition of **2c** at pH 2.0 and pH 7.0 is **8**, which was isolated and purified from the reaction mixture at pH 2.0 (Scheme 4). HPLC indicates that **8** is the only observable reaction product at all pH examined. At 30 °C **8** does not decompose to an observable extent except at pH 1.0, where it very slowly undergoes hydrolysis to hydroquinone, **9**. The other product, *tert*-BuOH, **12**, was detected by GC at pH 1.0 ((98 ± 4)%) and pH 7.0 ((87 ± 4)%). It appears that **2c** undergoes acid-catalyzed and uncatalyzed C−C bond cleavage to generate the *tert*-butyl cation, (or an E2 elimination with solvent H_2O as the base) but does not lose AcO^- to generate **1c**. The *tert*-butyl cation has a very short lifetime in H_2O, on the order of 10^{-12} s, so reaction with solvent would occur on an ion−molecule or ion pair rather than the free ion.[18] The analogous reaction of **2b** to form **8** as a minor product is unlikely to proceed through the isopropyl cation but could proceed by an E2 elimination. An S_N2 reaction is unlikely since **2a** does not generate **8**.

At pH 4.5 and 50 °C in 1/1 N_3^-/HN_3 buffers, **2c** decomposes without rate acceleration at $[N_3^-] \leq 0.25$ M with an average rate constant of $(6.7 \pm 0.3) \times 10^{-5}$ s^{-1}. The initial decomposition product **8** is detected by HPLC, but it decomposes into a new product that is generated after a noticeable delay time. This product is generated from the decomposition of authentic **8**, hydroquinone **9**, benzoquinone **10**, and 2-azidohydroquinone **13**[19] under the same conditions. The isolated product was identified as 2,3,5,6-tetraazidobenzoquinone**14**, on the basis of its IR and ^{13}C NMR spectra and by comparison to an authentic sample.[20] Since **14** is reported to be a dangerous explosive,[20,21] the compound was not purified, but the crude product is significantly more pure as isolated than the authentic sample produced by the reaction of NaN_3 with chloranil in EtOH.[20] No other N_3^--containing product was detected.

The reaction in N_3^-/HN_3 buffers indicates that decomposition of **2c** does not occur via an E2 elimination, since N_3^- is a stronger base than H_2O and would be expected to accelerate the elimination reaction. No acceleration of decomposition of **2c** is observed, although N_3^- accelerates the decomposition of **8**. The lack of N_3^--containing product other than **14** suggests that no minor pathway leading to **1c** occurs.

Sulfonamides similar to **4c** are known to require addition of TFA or TFSA to decompose in benzene,[9,11,12] but **4d** undergoes pH-independent decomposition in aqueous solution in the pH range 1−7 with no acid catalysis.[16] At pH > 7.0 there is a decrease in the rate of decomposition of **4d** associated with ionization of the substrate.[16] The sulfonamide **4c** shows the same behavior (Figure 2). Kinetic data for **4c** at 50 °C were fit to eq 4, the same equation previously used to fit the rate data for **4d**.[16]

$$\text{For } \mathbf{4c}\text{: } k_{obs} = ([H^+]/(K_a + [H^+]))k_o + (K_a/(K_a + [H^+]))k_- \quad (4)$$

The apparent pK_a of 8.3 ± 0.1 obtained from the kinetic fit was verified by spectrophotometric titration of **4c**. A plot of initial absorbance of **4c** at 205 nm versus pH (Figure S1 in the Supporting Information) yields a pK_a of 8.5 ± 0.2. In eq 4, k_o is the rate constant for spontaneous decomposition of **4c**, and k_- is the rate constant for decomposition of its conjugate base, **4c**$^-$.

The decomposition of **4c** at 50 °C yields three products: the rearranged sulfonamide **15**, 4-*tert*-butylphenol **16**, and 4-*tert*-butylcatechol **17** (Scheme 5). At pH ≤ 7.0, **15** is the major reaction product [(67 ± 11)%], while **16** [(19 ± 2)%], and **17** [(10 ± 4)%] are minor products. At higher pH, **15** is subject to decomposition so its yield cannot be determined accurately. The other two products are stable to the reaction conditions. The yield of the catechol **17** decreases as pH increases. It cannot be detected at pH > 8.2. The yield of the phenol **16** increases as pH increases and reaches a yield of (68 ± 4)% at pH 9.2. A plot of product yields versus pH is provided in Figure S2 in the Supporting Information. The data indicate that **16** is the major product of the decomposition of **4c**$^-$. This may be occurring by an α-elimination process (Scheme 5) to yield the known nitrene **18**, but it is unlikely that the significant amount of **16** detected at acidic pH is produced by such a process.[22,23] Decomposition of neutral **4c** leads predominantly to the rear-

(18) Toteva, M. M.; Richard, J. P. *J. Am. Chem. Soc.* **1996**, *118*, 11434−11445.

(19) Couladouros, E. A.; Plyta, Z. F. Haroutounian S. A. Papageorgiou, V. P. *J. Org. Chem.* **1997**, *62*, 6−10.

(20) Winkelman, E. *Tetrahedron* **1969**, *25*, 2427−2454.

(21) Gilligan, W. H.; Kamlet, M. J. *Tetrahedron Lett.* **1978**, 1675−1676.

(22) (a) Lwowski, W.; Maricich, T. J.; Mattingly, T. W., Jr. *J. Am. Chem. Soc.* **1963**, *85*, 1200−1202. (b) Lwowski, W.; Maricich, T. J. *J. Am. Chem. Soc.* **1965**, *87*, 3630−3637.

SCHEME 5. Products of the Decomposition of 4c with Possible Mechanisms

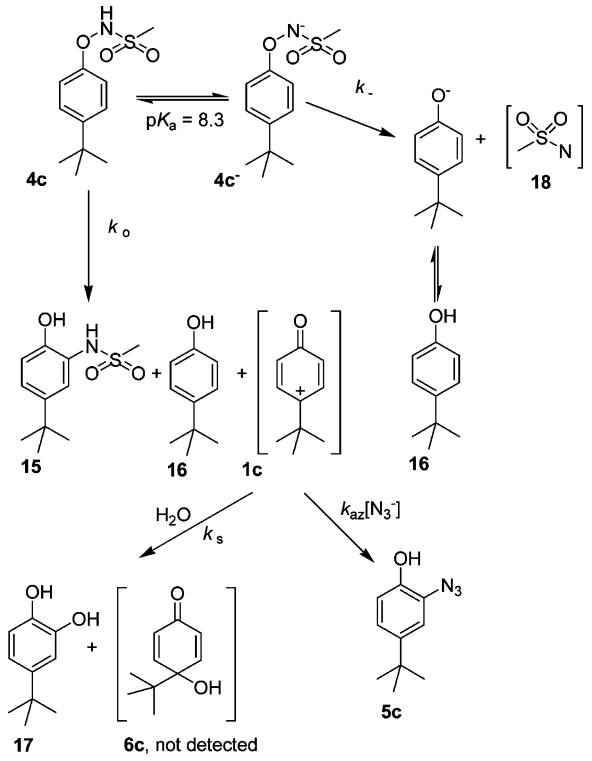

rangement product **15**, which may be generated by a concerted process or by internal return of an ion pair.[24,25] We are investigating the mechanisms of formation of the rearrangement product and the phenol in more detail in a different reaction system.[26]

The catechol **17** could be obtained from attack of H_2O on **1c**. By analogy to **1d** and other 4-aryl-substituted aryloxenium ions, one would have expected to obtain the quinol, **6c**, as the major product of attack of solvent.[14−16] Neither **6c** nor its expected dienone−phenol rearrangement product, *tert*-butylhydroquinone, were detected by HPLC in reaction mixtures of **4c**. The steric bulk of the *tert*-butyl group might alter the preferred site of attack of H_2O. If **1c** is formed, it should be possible to trap it with N_3^-. Figures 6 and 7 summarize the results of N_3^--trapping experiments performed in phosphate buffer at pH 7.0. In the absence of N_3^-, all products are formed in a first-order fashion. Under our HPLC conditions **4c** and **16** coelute, but the HPLC peak area for the combined peak containing both components is fit by a first-order rate equation as expected. In the presence of 0.45 M N_3^-, the yields of all products are altered to some extent and one new product, **5c**, is detected. The overall rate of reaction appears to be unaffected by the presence of N_3^- and all products are still produced in a first-order manner. The percentage yield of **15** decreases from ca. 54% to 42% in the presence of N_3^- and the yield of **16** increases by about half that amount, from ca. 17% to 24%. The

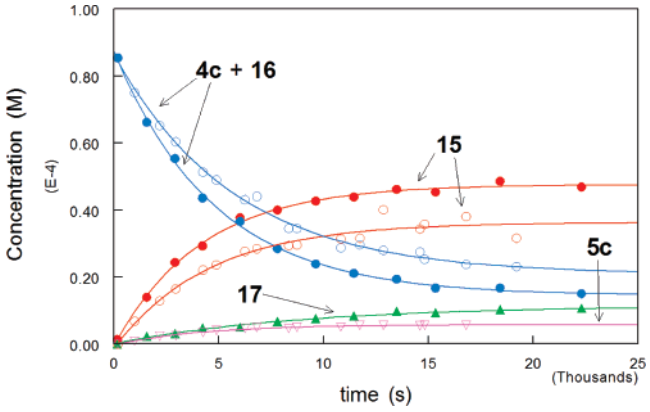

FIGURE 6. Concentration of products vs time during the decomposition of **4c** at pH 7.0 and 50 °C in the presence of 0.45 M N_3^- (open symbols) and in its absence (solid symbols).

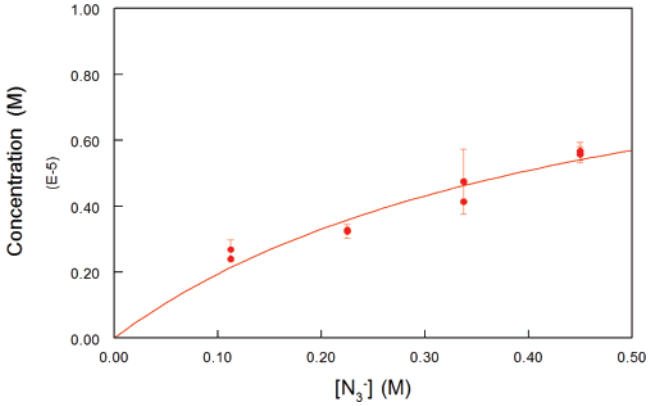

FIGURE 7. Yield of **5c** obtained from the reaction of **4c** at pH 7.0 and 50 °C as a function of [N_3^-]. Data were fit to eq 5.

relative effect on the yield of **17** is the largest. The HPLC peak for this compound is quite small and is partly obscured by the large N_3^- peak, but the yield of this compound has decreased from ca. 13% to less than 5% in the presence of N_3^-. The N_3^- adduct **5c** is easy to detect in the presence of N_3^- because it has a long retention time. Its yield is ca. 6% in the presence of 0.45 M N_3^-.

Figure 7 shows that the yield of **5c** depends on [N_3^-] in the concentration range 0−0.45 M. The yield of **5c** was fit by eq 5, where S is the observed azide/solvent selectivity and $[\mathbf{5c}]_{max}$ is the maximum yield of **5c** at infinite [N_3^-]. It can be shown that $S \geq k_{az}/k_s$, the ratio of the second-order rate constant for trapping of the free cation by N_3^- and the pseudo-first-order rate constant for trapping of the ion by the solvent (Scheme 5).[25]

$$[\mathbf{5c}] = ([\mathbf{5c}]_{max})(S[N_3^-])/(1 + S[N_3^-]) \qquad (5)$$

The data are adequately fit by eq 5 with $S = 2.1 \pm 0.8$ M^{-1} and $[\mathbf{5c}]_{max} = (1.1 \pm 0.3) \times 10^{-5}$ M, or (13 ± 3)%. Trapping by N_3^- accounts for only a small part of the overall reaction of **4c** and is also inefficient for the fraction of the path that is trapped.

For long-lived, highly selective ions $S = k_{az}/k_s$, but for unstable species with short aqueous solution lifetimes (<1 ns) the majority of the trapping occurs via a preassociation

(23) (a) Wasserman, E.; Smolinsky, G.; Yager, W. A. *J. Am. Chem. Soc.* **1964**, *86*, 3166−3167. (b) Moriarty, R. M.; Rahman, M.; King, G. J. *J. Am. Chem. Soc.* **1966**, *88*, 842−8433. (c) Abramovitch, R. A.; Knaus, G. N.; Uma, V. *J. Am. Chem. Soc.* **1969**, *91*, 7532−7533.

(24) Oae, S.; Sakurai, T. *Tetrahedron* **1976**, *32*, 2289−2294.

(25) Novak, M.; Kahley, M. J.; Lin, J.; Kennedy, S. A.; James, T. G. *J. Org. Chem.* **1995**, *60*, 8294−8304.

(26) Y. Wang and M. Novak, work in progress.

SCHEME 6. Isodesmic Reaction of 4-Substituted Aryloxenium Ions

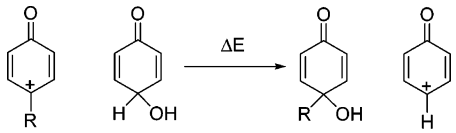

1 a R = Me
b R = iPr
c R = *t*-Bu
d R = 4-MePh
e R = Ph

6 a R = Me
b R = iPr
c R = *t*-Bu
d R = 4-MePh
e R = Ph

TABLE 2. Calculated Values of Δ*E* for 1a−e and Extrapolated k_{az}/k_s for 1a−c

ion	Δ*E* (kcal/mol) HF/6-31G*	Δ*E* (kcal/mol) B3LYP/6-31G*//HF/6-31G*	extrapolated k_{az}/k_s (M^{-1})
1a	10.6	11.2	1.8×10^{-3}
1b	16.0	16.6	3.8×10^{-2}
1c	15.2	16.0	2.8×10^{-2}
1d	30.6	35.4	
1e	25.9	30.3	

mechanism and $S > k_{az}/k_s$.[18,25,27] For the present case, since the N_3^- trapping accounts for such a small part of the reaction of **4c**, it is not possible to unequivocally state that an oxenium ion has been trapped. Rate changes that could distinguish between trapping of an intermediate generated after a rate-limiting step or direct reaction on **4c** are within the error limits of the kinetics measurements when trapping amounts to <10% of the overall reaction. If the oxenium ion **1c** is trapped, k_{az} must be diffusion-limited at ca. 10^{10} M^{-1} s^{-1} at 50 °C for such a reactive species, and k_s is $\geq 0.5 \times 10^{10}$ s^{-1}. The lifetime ($1/k_s$) of the putative ion is no more than 0.2 ns if the reaction occurs through a free ion. In contrast, **1d** has an estimated lifetime of ca. 170 ns at 30 °C based on N_3^- trapping[16] The azide/solvent selectivity for **1c** is in the range in which a significant amount of the trapping occurs via preassociation.[18,25,27] The lifetime estimate of 0.2 ns for **1c** must be considered an upper limit since it cannot be established that the trapping actually occurs on the ion, and if an ion is involved a significant part of the trapping must occur by preassociation. For nitrenium ions with similar azide/solvent selectivity, the lifetime of the "free" ion is approximately an order of magnitude less than calculated from the experimental azide/solvent selectivity.[25] This would suggest that the lifetime of "free" **1c** is no larger than ca. 20 ps. This is similar to the estimates of 3−5 ps for **1a** based on earlier density functional theory (DFT) calculations and kinetic extrapolations of ions with known lifetimes.[15]

The isodesmic reaction of Scheme 6 has proven to be a useful tool for the correlation of experimental and calculated properties of oxenium ions.[15−17] Δ*E* for the reaction provides the calculated driving force for hydration of 4-substituted aryloxenium ions to form the corresponding quinols, **6**, relative to the unsubstituted ion. Δ*E* values calculated at the HF/6-31G* and B3LYP/6-31G*//HF/6-31G* levels for ions **1a**−**e** are presented in Table 2. We have previously shown that singlet−triplet energy gaps and structures of para-substituted arylnitrenium ions calculated by DFT methods on HF/6-31G* geometries are comparable to those calculated on the same ions with full DFT optimization on a correlation-consistent polarized valence double-ζ basis set, BPW91/cc-pVDZ.[17,28] This is due, at least in part, to limited configuration interaction caused by the relatively large singlet−triplet energy gap in these ions.[17] This is also true for similarly substituted aryloxenium ions.[17] It appears that the B3LYP/6-31G*//HF/6-31G* calculations provide useful results, particularly when applied to isodesmic reactions.[15−17] We have previously shown that zero-point energy (ZPE) and thermodynamic corrections to Δ*E* largely cancel, so they have not been included in these calculations.[15,17] The results shown in Table 2 suggest that electron correlation effects also largely cancel, as previously observed.[15−17]

The 4-alkyl-substituted ions **1a**−**c** are clearly significantly destabilized compared to **1d** and **1e**, although the isopropyl and *tert*-butyl substituents of **1b** and **1c** apparently provide marginal stabilization (ca. 5 kcal/mol) for hydration of these two species. We have previously noted that 4-aryl substituents have a significant stabilizing effect on aryloxenium ions.[15,16] A previously published correlation of observed log (k_{az}/k_s) at 30 °C versus Δ*E* at the B3LYP/6-31G*//HF/6-31G* level for four 4-aryl-substituted aryloxenium ions including **1d** and **1e** provides a means to extrapolate k_{az}/k_s for **1a**−**c**.[16] The extrapolation provides the values shown in Table 2. The measured k_{az}/k_s for the ions used in the correlation are in the range from ca. 10^2 to 10^5 M^{-1}, and Δ*E* at the B3LYP/6-31G*//HF/6-31G* level for those ions are in the range 29−43 kcal/mol, so the extrapolation is quite long. Assuming that k_{az} is diffusion-limited at ca. 6×10^9 M^{-1} s^{-1},[14] the estimated lifetimes ($1/k_s$) of **1a** (0.3 ps), **1b** (6 ps), and **1c** (5 ps) are too short by 2−3 orders of magnitude to be diffusionally trapped by a non-solvent nucleophile.[18,25,27] The estimated lifetime of **1a** is about 10-fold shorter than we have previously estimated by two other kinetic extrapolations.[15,29] These lifetime estimates have an error limit of at least an order of magnitude, but they do indicate that simple 4-alkylaryloxenium ions are fleeting and unselective species in water that will react only with nucleophiles that are present in the solvation shell in which they are generated.[18,25,27] The calculations also suggest that the reason precursors such as **2a**−**c**, **3a,b**, and **4c** do not efficiently generate 4-alkylaryloxenium ions while **2d**, **4d**, and similar compounds do generate 4-arylaryloxenium ions is due to the significant stabilization provided to the latter species by the 4-aryl substituent.

Conclusion

The putative oxenium precursors **2b**, **2c**, **3b**, and **4c** exhibit a variety of chemistry, but with one possible exception, they do not generate an oxenium ion. The 4-isopropyl ester **2b**, similar to its 4-methyl analogue **2a**, reacts predominantly by ordinary ester hydrolysis, while the 4-*tert*-butyl ester **2c** apparently generates the *tert*-butyl cation by acid-catalyzed and uncatalyzed pathways. The 4-isopropyl ester with the dichloroacetate leaving group, **3b**, generates the oxenium-like N_3^- trapping product **5b** but does so by a kinetically bimolecular path that does not involve an oxenium ion. The sulfonamide **4c**

(27) Novak, M.; Rajagopal, S. *Adv. Phys. Org. Chem.* **2001**, *36*, 167−254.

(28) Sullivan, M. B.; Brown, K.; Cramer, C. J.; Truhlar, D. G. *J. Am. Chem. Soc.* **1998**, *120*, 11778−11783.

(29) A reviewer has suggested that solvation effects might significantly alter the extrapolations of these kinetic correlations. In a preliminary study we added the AM1 SM5.4 aqueous solvation energies to the B3LYP/6-31G*//HF/6-31G* energies of **1** and **6** in Scheme 6. The correlation of the four original ions was not significantly altered, and the long extrapolation to **1a**−**c** led to modest changes in the estimated lifetime of these ions: 1.7 ps for **1a**, 12.8 ps for **1b**, and 3.3 ps for **1c**. These lifetime estimates do not change our original conclusions.

may generate the oxenium ion **1c** via a minor decomposition pathway, but if the ion is generated, its aqueous solution lifetime is in the range of 20−200 ps. Many of the cases in which oxenium ions have been invoked to explain reaction products have involved alkyl-substituted ions in nucleophilic solvents such as H_2O or MeOH.[1−13] In view of our results, alternative mechanisms should be considered in these cases.

Experimental Section

Synthesis of compounds **2b**, **2c**, **3b**, and **4c** followed procedures that we have published for related materials.[14−16] Details of the synthesis, purification, and characterization of these materials can be found in the Supporting Information.

Isolation, Purification, and Characterization of Reaction Products. Four azide-containing products were isolated from large-scale decomposition reactions in buffers containing N_3^-: **5b**, **5c**, **11b**, and **14**.

Products 5b and 11b. A 136 mg sample of **3b** (0.52 mmol) was dissolved in 1 mL of dry CH_3CN. This solution was added in 0.1 mL aliquots every 3 h to 1 L of a 5 M 1/1 NaN_3/HN_3 buffer containing 5 vol % CH_3CN that was incubated at 30 °C in a shaker bath. (Caution: HN_3 is nearly saturated under these conditions. The reaction flask should be kept stoppered in a well-ventilated location, and inhalation of toxic HN_3 should be avoided.) The reaction mixture was neutralized with solid $NaHCO_3$ to a pH of 6.5 when HPLC indicated that the reaction was complete (48 h). The aqueous reaction mixture was extracted with CH_2Cl_2 (5 × 100 mL). The combined organic extracts were dried over Na_2SO_4, filtered, and evaporated on a rotary evaporator at ambient temperature to yield 95 mg of crude product. This material was applied to a 2 mm silica gel chromatatron plate and eluted with CH_2Cl_2. Two azide-containing materials were isolated: 20 mg of **5b** and 12 mg of **11b**. 2D NMR data and complete NMR assignments for both compounds are presented in the Supporting Information.

2-Azido-4-isopropylphenol (5b). mp 43−44 °C; IR 3425, 2960, 2104, 1600, 1510, 1300, 1249, 1195 cm^{-1}; ^1H NMR (500 MHz, CD_2Cl_2) δ 1.22 (6H, d, J = 6.9 Hz), 2.86 (1H, septet, J = 6.9 Hz), 5.22 (1H, s), 6.82 (1H, d, J = 8.3 Hz), 6.92 (1H, dd, J = 1.8, 8.2 Hz), 6.95 (1H, d, J = 2.1 Hz); ^{13}C NMR (125.8 MHz, CD_2Cl_2) δ 24.2, 33.9, 116.0, 116.7, 124.3, 125.9, 142.6, 145.7; LC/MS (APCI, positive) *m*/*e* 150 (100%) (M + H − N_2); high-resolution MS (ES, positive) $C_9H_{11}N_3ONa$ (M + Na) calcd 200.0800, found 200.0800.

3-Azido-4-isopropylphenol (11b). mp 54−55 °C; IR 3333, 2963, 2110, 1609, 1591, 1504, 1297, 1218 cm^{-1}; ^1H NMR (500 MHz, CD_2Cl_2) δ 1.16 (6H, d, J = 6.9 Hz), 3.11 (1H, septet, J = 6.9 Hz), 4.98 (1H, s), 6.59 (1H, dd, J = 2.5, 8.4 Hz) 6.63 (1H, d, J = 2.4 Hz), 7.10 (1H, d, J = 8.4 Hz); ^{13}C NMR (125.8 MHz, CD_2Cl_2) δ 23.1, 27.7, 105.5, 112.4, 127.9, 132.8, 138.5, 154.9; LC/MS (APCI, positive) *m*/*e* 150 (100%) (M + H − N_2); high-resolution MS (ES, positive) $C_9H_{11}N_3ONa$ (M + Na) calcd 200.0890, found 200.0794.

Product 5c. A 100 mg sample of **4c** (0.5 mmol) was dissolved in 10 mL of dry CH_3CN. This solution was added over 4 h via syringe pump to 1 L of a 0.02 M phosphate buffer, pH 7.0, containing 5 vol % CH_3CN and 0.45 M NaN_3 that was incubated in a shaker bath at 50 °C. The reaction mixture was extracted (4 × 100 mL) with CH_2Cl_2 when HPLC indicated that the reaction was complete (10 h). The combined extracts were dried over Na_2SO_4, filtered, and evaporated at ambient temperature on a rotary evaporator. The residue was applied to a 2 mm silica gel chromatatron plate and eluted with 95/5 CH_2Cl_2/EtOAc. One azide-containing product was isolated: 4 mg of **5c**.

2-Azido-4-*tert*-butylphenol (5c). Yellow to brown oil; IR 3300, 2963, 2119, 1514 cm^{-1}; ^1H NMR (300 MHz, CD_2Cl_2) δ 1.33 (9H, s), 5.25 (1H, br s), 6.86 (1H, d, J = 8.6 Hz) 7.08−7.12 (2H, m); ^{13}C NMR (75.5 MHz, CD_2Cl_2) δ 31.5, 34.7, 115.6, 115.9, 123.4, 125.5, 145.0, 145.4; LC/MS (APCI, positive) *m*/*e* 164 (100%) (M + H − N_2); high-resolution MS (ES, positive) $C_{10}H_{13}N_3ONa$ (M + Na) calcd 214.0956, found 214.0951.

Product 14. A 50 mg sample of 2-azidohydroquinone **13**[18] (0.33 mmol) was dissolved in 1 mL of dry CH_3CN. This solution was added in 0.1 mL aliquots every 0.5 h to 0.5 L of a 0.5 M 1/1 NaN_3/HN_3 buffer containing 5 vol % CH_3CN that was incubated at 50 °C in a shaker bath. The mixture was periodically monitored by HPLC. After 12 h the reaction mixture was refrigerated overnight and then brought back to room temperature the next day. HPLC showed the peak for the product continued to increase in intensity during the day. The sample was refrigerated overnight and brought back to room temperature during the day for 5 days until HPLC indicated that the product peak had reached maximum intensity. The reaction mixture was then neutralized to a pH of 7 with saturated aqueous $NaHCO_3$ and extracted (3 × 100 mL) with CH_2Cl_2. The combined extracts were dried over Na_2SO_4, filtered, and evaporated to dryness on a rotary evaporator to yield 25 mg of a blue-black solid. TLC on silica gel with CH_2Cl_2 eluent indicated one major component, as did HPLC analysis. HPLC analysis showed that the isolated product had the same retention time as the material obtained from the reaction mixtures of **2c** in N_3^- solutions.

2,3,5,6-Tetrazido-1,4-benzoquinone (14). Blue-black solid; IR 2105, 1662, 1581, 1327 cm^{-1}; ^{13}C NMR (125.8 MHz, CD_2Cl_2) δ 126.7, 176.1. The compound is described in the literature, but IR and NMR data have not been previously reported.[20,21] A sample prepared from chloranil according to the literature procedure[20] has the same IR and ^{13}C NMR peaks as the compound isolated from the product study but is significantly less pure. Since the compound is reported to be highly explosive,[20,21] and scratching of 5 mg of the sample prepared from chloranil on a glass plate led to a spark and an audible pop, no further attempts to purify either sample were made.

Reaction products that did not contain azide, **6b**, **8**, **15**, **16**, and **17**, were isolated from large-scale decomposition reactions. Products **8**, **16**, and **17** were identified by direct IR and NMR comparison to authentic samples. Hydroquinone **9**, and benzoquinone **10** were not isolated but were identified by HPLC retention time comparisons to authentic materials. Isolation, purification, and characterization of **6b** and **15** are described below.

Product 6b. A 50 mg sample of **3b** (0.19 mmol) was dissolved in 1 mL of dry CH_3CN. This solution was added in 0.1 mL aliquots every 15 min to 250 mL of a 0.02 M phosphate buffer, pH 7.45, containing 5 vol % CH_3CN that was incubated at 30 °C in a water bath. The reaction mixture was incubated for an additional 3 h after addition of the last aliquot of **3b**. The reaction mixture was extracted (5 × 50 mL) with CH_2Cl_2. The combined extracts were dried over Na_2SO_4, filtered, and evaporated to dryness on the rotary evaporator to yield 25 mg of an off-white solid that was sufficiently pure for characterization.

4-Hydroxy-4-isopropyl-2,5-cyclohexadienone (6b). mp 70.5−71.5 °C; IR 3337, 2963, 1655, 1615, 971 cm^{-1}; ^1H NMR (300 MHz, CD_2Cl_2) δ 0.95 (6H, d, J = 6.9 Hz), 2.06, (1H, septet, J = 6.9 Hz), 2.09 (1H, s), 6.18, (2H, d, J = 10.2 Hz), 6.80 (2H, d, J = 10.2 Hz); ^{13}C NMR (75.5 MHz, CD_2Cl_2) δ 17.0, 37.1, 72.6, 129.3, 150.5, 185.9; LC/MS (APCI, positive) *m*/*e* 135 (100%) (M + H − H_2O); high-resolution MS (ES, positive) $C_9H_{12}O_2Na$ (M + Na) calcd 175.0735, found 175.0733.

Product 15. A 100 mg sample of **4c** (0.41 mmol) was dissolved in 2 mL of dry CH_3CN. This solution was added in 0.2 mL aliquots every 50 min to 500 mL of a 0.02 M phosphate buffer, pH 6.6, containing 5 vol % CH_3CN that was incubated in a water bath at 50 °C. The reaction mixture was incubated overnight after addition of the last aliquot of **4c**. The mixture was extracted (5 × 50 mL) with CH_2Cl_2. The combined extracts were dried over Na_2SO_4, filtered, and evaporated to dryness on the rotary evaporator. The residue was applied to a 2 mm silica gel chromatatron plate and eluted with 90/10 CH_2Cl_2/EtOAc. The fraction containing **15**

yielded 55 mg of a white solid that was sufficiently pure for characterization.

***N*-(5-*tert*-Butyl-2-hydroxyphenyl)methanesulfonamide (15).** mp 145−147 °C; IR 3382, 3297, 2954, 1615, 1514, 1382, 1303, 1288, 1130, 1124 cm^{-1}; ^1H NMR (300 MHz, CD_2Cl_2) δ 1.29 (9H, s), 2.98 (3H, s), 6.2 (2H, br s), 6.90 (1H, d, $J = 8.3$ Hz) 7.21 (1H, dd, $J = 2.3$, 8.4 Hz), 7.24 (1H, d, $J = 2.1$ Hz); ^{13}C NMR (75.5 MHz, CD_2Cl_2) δ 31.5, 34.5, 38.9, 116.9, 122.9 123.0, 125.7, 145.2, 148.3; LC/MS (ESI, positive) *m*/*e* 266 (80%) (M + Na), 165 (100%) (M + H − SO_2CH_3); LC/MS (ESI, negative) *m*/*e* 242 (100%) (M − H); high-resolution MS (ES, positive) $C_{11}H_{17}NO_3SNa$ (M + Na) calcd 266.0827, found 266.0823.

Kinetics and Product Analyses. All kinetics were run in 5 vol % CH_3CN-H_2O at $\mu = 0.5$ ($NaClO_4$) in $HClO_4$ solutions (pH < 3.0), or in 0.02 M $HCO_2H/NaHCO_2$, AcOH/AcONa, NaH_2PO_4/Na_2HPO_4, or $TrisH^+$/Tris buffers at 30 °C (**2c**, **3b**), 50 °C (**4c**), or 80 °C (**2b**). Reactions were initiated by injection of 15 μL of a 0.01−0.02 M stock solution of the desired compound in dry CH_3CN into 3 mL of the reaction solution that had been incubated at the appropriate temperature for at least 15 min. UV absorption versus time data were taken at 244 nm for **2b**; at 240, 247, and 255 nm for **2c**; at 220 and 240 nm for **3b**; and at 205 and 224 nm for **4c**. HPLC data were monitored at 240 nm for **2b**, **2c**, and **3b** and at 220 nm for **4c**. Other HPLC conditions were C-8 reverse-phase column, 50/50−60/40 MeOH/H_2O, 1 mL/min flow rate, 20 μL injections. These same HPLC conditions were used for product analyses at the end of kinetic runs and during isolation experiments. Most UV and HPLC data were fit by nonlinear least-squares methods to the standard first-order rate equation. If initial reaction products were unstable, UV absorbance and HPLC peak area data for the unstable product were fit to the standard equation for consecutive first-order reactions. HPLC peak area data for the reactants always fit the first-order rate equation well, as did UV absorbance data for cases in which the products were stable. HPLC was always used to verify the magnitude of the rate constant for disappearance of the reactant (k_{obs}) in cases in which the UV absorbance data had to be fit to the consecutive first-order rate equation. Rate constants for very slow reactions ($k_{obs} < 5 \times 10^{-6}$ s^{-1}) were determined by fitting UV absorbance or HPLC peak area versus time for the first 5% of the reaction to a linear equation and dividing the slope by either the total UV absorbance change or by the initial HPLC peak area. The experimental conditions and calculation methods for each rate constant obtained are provided in Tables S1−S4 in the Supporting Information.

Detection and quantification of *tert*-butanol, **12**, generated during the decomposition of **2c** was performed by gas chromatography with the following GC conditions: 0.25 mm × 30 m VF-35ms column, 2 μL injections at 250 °C and 5/1 split, initial 50 °C column for 5 min increasing by 10 °C/min to 250 °C, 0.3 mL/min flow rate, FID detection with 250 °C detector oven, *n*-decanol internal standard. Reactions were run at pH 1.0 and 7.0 in solutions identical to those used for kinetics except that CH_3CN was not included. Reaction was initiated by adding sufficient solid **2c** to 2 mL of the reaction mixture stirred in a 5 mL conical vial to bring the initial concentration to ca. 2×10^{-2} M. Reaction mixtures were incubated at 30 °C, and the reaction was monitored by HPLC. Control experiments with 2×10^{-2} M **12** were run at the same time. When **2c** had disappeared from the reaction mixture according to HPLC, the reaction and control mixtures were cooled to room temperature, *n*-decanol (2×10^{-2} M) was added followed by 0.30 g of NaCl, and the aqueous mixtures were extracted with 2 mL of CH_2Cl_2. The organic extract was removed to a separate conical vial by pipet, dried over Na_2SO_4, and kept tightly sealed until GC analysis that was initiated within 20 min of completion of extraction. Duplicate injections of each sample were averaged. All data were corrected to the internal standard, and yields were determined by comparison of the corrected peak areas for **12** in the experimental and control run.

Calculations. Detailed descriptions of the calculation methods have been published.[17] Geometries and energies for **1a**, **1d**, **1e**, **6a**, **6d**, and **6e** have been published.[15,16] The same procedures were followed for **1b**, **1c**, **6b**, and **6c** utilizing Spartan 04 for Macintosh Version 1.0.1 and Spartan Version 5.[30] Geometries were optimized at the HF/6-31G* level. Frequency analyses were performed at this level to verify that all geometries corresponded to true stationary points. These geometries were used to obtain energies at the density functional level B3LYP/6-31G*//HF/6-31G*. Optimized HF/6-31G* geometries and energies at all levels calculated for **1b**, **1c**, **6b**, and **6c** are presented in the Supporting Information.

The isodesmic reaction of Scheme 6 was used to evaluate the hydration energies of **1a**−**e** relative to the parent phenyloxenium ion. Calculations of isodesmic reactions were carried out by use of (1) HF/6-31G* energies without electron correlation or (2) B3LYP/6-31G*//HF/6-31G* with electron correlation.

Acknowledgment. We thank the Donors of the American Chemical Society Petroleum Research Fund for support of this research (Grant 43176-AC4). The 500 MHz NMR spectrometer and the LC/MS were provided by grants to Miami University by the Hayes Investment Fund of the Ohio Board of Regents. J.N.D. received a summer research internship from the Department's NSF-REU grant. J.M.E. received a grant for research supplies from Miami's Undergraduate Research Awards Program.

Supporting Information Available: Synthesis and characterization of **2b**, **2c**, **3b**, and **4c**; Tables S1−S4, containing rate constants for all reactions of **2b**, **2c**, **3b**, and **4c**; complete ^1H and ^{13}C NMR assignments for **5b** and **11b**; Figure S1, spectrophotometric titration of **4c**; Figure S2, product yields for the decomposition of **4c** as a function of pH; ^1H and ^{13}C NMR spectra for **2b**, **2c**, **3b**, **4c**, **5b**, **5c**, **6b**, **11b**, **14**, and **15**; and optimized geometries for **1b**, **1c**, **6b**, and **6c** at the HF/6-31G* level with energies at the HF/6-31G* and B3LYP/6-31G*//HF/6-31G* levels. This material is available free of charge via the Internet at http://pubs.acs.org.

JO701853E

(30) Wavefunction, Inc., 18401 Van Karman Ave., Suite 370, Irvine, CA, 92612.